Chemical Engineering Journal 162 (2010) 776–786

Contents lists available at ScienceDirect

Chemical Engineering Journal

journal homepage: www.elsevier.com/locate/cej

Isothermal and non-isothermal polymerization of methyl methacrylate in presence of multiple initiators

Marco Biondi[1], Assunta Borzacchiello[2], Paolo Antonio Netti[*,1]

Department of Materials and Production Engineering, University of Naples Federico II, Piazzale Tecchio 80, 80125 Naples, Italy

ARTICLE INFO

Article history:
Received 29 July 2009
Received in revised form 3 June 2010
Accepted 5 June 2010

Keywords:
Kinetic modeling
Initiators
Bulk free radical polymerization

ABSTRACT

Methyl methacrylate (MMA) polymerization is a diffusion-controlled reaction, characterized by a strong gel effect, which may cause uncontrolled heat generation and the thermal runaway of the process. For applications to industrial polymerization, kinetic control is particularly important and difficult to achieve due to the interplay between heat development and diffusional control occurring during polymerization. Sustaining the polymerization reaction (i.e. enhancing heat exchange) is a promising strategy to control MMA polymerization kinetics. In particular, different initiators triggering polymerization at different times can be used, thus reducing the possibility of thermal runaway by engineering temperature history and initiator nature/concentrations. There are few models accounting for the presence of multiple initiators and non-isothermal conditions. Therefore, a new, simple semi-empirical model, relating degree of conversion and polymerization rate to time and temperature, was developed. To validate the model, DSC tests were performed in isothermal and non-isothermal conditions, thus deriving the heat developed during polymerization. Model parameters were calculated from isothermal DSC experiments, and the model was predictive of monomer conversion in non-isothermal conditions in presence of single initiators and the mixture of them. Results indicate that, by varying formulation parameters (temperature history and initiator concentrations), polymerization kinetics may be optimized.

1. Introduction

Bulk free radical polymerization is a versatile process, which can be carried out on many monomers and in a wide range of temperatures. Free radical polymerization occurs in three steps, namely initiation (formation of free radicals because of initiator fragmentation), propagation (shifting of the reacting site on the chain end during monomer conversion) and termination, and is characterized by a strong increase of the system viscosity while the monomer is converted. In these conditions significant changes of mass and heat transfer occur. The reaction is characterized, especially at high monomer conversions, by conversion-related diffusional hindrances of the different reacting species, namely gel (or Trommsdorff), glass and cage effects [1–6]. Gel effect is related to the selective reduction of termination over propagation rate as termination step occurs when two growing (macro)radicals collide, and is therefore more sensitive to the mobility of macromolecules, while no appreciable effect on monomer mobility takes place. The net effect is a sharp increase in polymerization rate/heat generation, due to incipient macromolecular entanglement. Gel effect is particularly apparent in the bulk polymerization of methyl methacrylate (MMA), and is highly undesired in industrial applications as may lead to the thermal runaway of the process, thus causing depolymerization and plugging of equipment [1,7,8]. Glass effect occurs because glass transition temperature of the reacting mixture (T_g) increases with increasing monomer conversion. When T_g equals polymerization temperature, also monomer mobility is reduced thus hindering also propagation events. In these conditions, occurring at later conversion stages, monomer diffusion is hindered, and the reacting solution anneals before 100% monomer conversion due to an extreme increase of the medium viscosity [2,9–11]. Finally, cage effect occurs when even the mobility of initiator radicals is hindered, thus preventing initiation events. This is detrimental to initiator efficiency, and affects monomer conversion and polymer molecular weight [11–14]. Glass and cage effects take place when polymerization is carried out at temperatures lower than the T_g of the polymer, which makes the diffusional control predominant.

In the case of MMA polymerization for industrial applications, the kinetic control is particularly important since chemical reac-

* Corresponding author. Current address: Interdisciplinary Research Centre on Biomaterials (CRIB), University of Naples Federico II, Piazzale Tecchio 80, 80125 Naples, Italy/Italian Institute of Technology (IIT), via Morego 30, 16163 Genoa, Italy. Tel.: +39 0817682408; fax: +39 0817682404.
E-mail address: nettipa@unina.it (P.A. Netti).
[1] Current address: Interdisciplinary Research Centre on Biomaterials (CRIB) University of Naples Federico II, Piazzale Tecchio 80, 80125 Naples, Italy/Italian Institute of Technology (IIT), via Morego 30, 16163 Genoa, Italy.
[2] Current address: Institute of Composite and Biomedical Materials, CNR and CRIB, University of Naples Federico II, Piazzale Tecchio 80, 80125 Naples, Italy.

1385-8947/$ – see front matter © 2010 Elsevier B.V. All rights reserved.
doi:10.1016/j.cej.2010.06.004

tion and shaping occur simultaneously. The kinetic control is very difficult to achieve due to the highly exothermic nature of the reaction and to the aforementioned diffusional obstacles occurring during polymerization. This leads to uncontrolled temperature growth, process instabilities, monomer loss/boiling and uneven molecular weight distribution, and induces residual stresses and voids resulting in worsening of product quality/process efficiency. In addition, these problems are more significant with increasing product dimension/decreasing surface:volume ratios.

The optimization of MMA polymerization relies on many engineering variables such as temperature history, feed concentrations, product size, process times and may improve commercial potential/product quality, also reducing waste generation and production costs [15–19]. The kinetic control of MMA polymerization may be achieved by sustaining the polymerization process, thus enhancing heat exchange. To this end, a possible strategy is the contemporary use of different initiators triggering initiator scission at different times with the aim of distributing heat generation, thus reducing the possibility of thermal runaway under an optimized temperature history [20–26]. In addition to this, nature and concentration of initiators, and thermal history of the reacting system, are crucial parameters for the optimization of MMA polymerization.

There is vast literature, based on fundamental and empirical approaches, dealing with gel and glass effects [27–30], together with reviews focused on process improvement by mathematical modeling [31–33]. Some models attempt to correlate kinetic constants [8,34,35], or transport properties of polymer and monomer [36–38] with conversion, temperature, free volume/chain end mobility [6,37–41], or to view chain growth as a statistical phenomenon leading to different states based on some relevant kinetic parameters, or on diffusion/reptation theories [42–48]. More recently, attention was paid to non-isothermal and semi-batch conditions, which are extremely important in the industrial practice [49–54]. Some models consider the presence of different initiators or mixture of initiators, and other models take into account non-isothermal conditions [25,45,55–60]. To our knowledge, however, results on the contemporary presence of multiple initiators and the presence of dynamic conditions are still few. It must also be underlined that empirical approaches are more successful compared to molecular modeling as reviewed by Tefera et al. [61,62].

In this context, the aims of this work were the quantification and the prediction of heat generation/conversion history during MMA polymerization in presence of multiple initiators and in both isothermal and dynamic conditions. A simple semi-empirical model relating two state variables (degree of conversion and polymerization rate) to time and temperature was developed. In particular, in this work both the simultaneous presence of different initiators, used in the industrial practice, and non-isothermal temperature profiles were contemporarily taken into account in a simple, semi-empirical model. To validate the model, DSC tests were performed in both isothermal and non-isothermal conditions and used to calculate the heat generation associated to monomer conversion. Model parameters were estimated after isothermal DSC experiments, while dynamic conditions were predicted by the model, without any fitting, in presence of single initiators and the mixture of them.

2. Experimental

2.1. Materials

MMA containing 0.1% terpinolene (Sigma–Aldrich, Italy) as a polymerization inhibitor, and poly(methyl methacrylate) (PMMA) were provided by Clax Italia (Italy). Three non peroxide initiators, ADVN 2,2′-azobis (2,4-dimethylvaleronitrile), AIBN 2,2′-azobis (isobutyronitrile), ACHN 1,1′-azobis (cyclohexanecarbonitrile), namely Vazo®52, Vazo®64 and Vazo®88, were purchased from DuPont (Canada). Vazo® initiators decompose with first-order kinetics and produce less energetic radicals compared to peroxides, so they induce less branching and cross-linking [63]. Grade numbers of Vazo® initiators represent the temperature, expressed in Celsius degrees at which initiator half-life (the time necessary for initiator concentration to decay to half of its initial value) in solution is 10 h. Vazo® initiators thermally decompose forming two primary radicals triggering MMA polymerization. The initiator concentrations employed for Vazo®52, Vazo®64, Vazo®88 were 5.25×10^{-5} mol/L MMA, 6.24×10^{-5} mol/L MMA, 1.14×10^{-4} mol/L MMA, respectively. These concentrations were chosen as they are used in the industrial practice and, to simulate the actual conditions, the same initiator concentrations were used for the experimental plan. In particular, it must be underlined that prolonged induction times are helpful for the system to reach thermal equilibrium before polymerization onset. The reactants were used as received.

2.2. Methods

To study the polymerization kinetics of MMA and determine the T_g of PMMA, differential scanning calorimetry (DSC) experiments were performed (2910 DSC, TA Instruments, Wilmington, DE, USA) under a constant 50 cm^3/min nitrogen flow. Samples were prepared at room temperature and inserted in hermetically sealed aluminum pans. Isothermal measurements were carried out for 3–20 h, depending on the temperature and the initiator used, between 60 and 90 °C (step: 5 °C).

To determine the unreacted monomer fraction and the T_g of the partially and completely cured polymer, two dynamic scans were performed after each isothermal test (temperature range: 40–180 °C; heating rates: 1 °C/min for the first scan; 10 °C/min for the second scan). In particular, T_g of the partially cured polymer was calculated as the point of the thermogram immediately preceding the onset of polymerization after the first scan. Indeed, in the case of diffusion-controlled reactions, the residual monomer can polymerize only when the system temperature exceeds the T_g of the reacting mixture. The T_g of the fully cured system was the temperature corresponding to the inflection point of the DSC thermogram obtained by the second dynamic scan.

To minimize monomer evaporation during experiments, kinetic tests were performed on a 30% (w/v) solution of PMMA in MMA. Dynamic experiments were carried out, in presence of one initiator, and with the mixture of the three Vazo®s, added with halved initial concentrations. Heating rate was 0.5 °C/min. The conversion and rate resulting from dynamic experiments were compared, without any fitting, to the predictions of the model obtained by using the parameters as derived from isothermal experiments after fitting to the experimental results. To assess mass conservation during DSC experiments, samples were weighed before and after each experiment, and the mass loss evaluated.

3. Kinetic modeling

MMA polymerization is a free radical chain reaction, which can be schematized in three steps: initiation, propagation and termination. The rate of monomer disappearance is considered to be coincident with the rate of polymerization, i.e. with the rate of propagation. If the quasi stationary state approximation (QSSA) holds, the concentration of radicals initially increases, but almost instantaneously reaches a steady value. Another basic assumption needed to build the model is the long chain hypothesis (LCH), which assumes that the radical chain is composed by a high num-

ber of monomer units. This leads to consider that the initiation step depends on the nature of the initiator, while propagation and termination are basically initiator-independent. Under these hypotheses, macroradical concentration can be considered steady during most of the reaction and the rate of monomer consumption is expressed by [1]:

$$-\frac{d[M]}{dt} = R_p = k_p[M][P\cdot] = k_p\left(\frac{fk_d}{k_t}\right)^{1/2}[I]^{1/2}[M], \quad (1)$$

where R_p is the overall rate of polymerization; $[M]$, $[P\cdot]$ and $[I]$ are the monomer, growing macroradical and initiator concentrations; k_d, k_t and k_p are the decomposition, termination and propagation rate constants, respectively; f is the initiator efficiency. To derive the kinetic expression, chain transfer was neglected as it is more likely to occur in solution polymerization, while in this work bulk MMA polymerization is considered [47]. Eq. (1) can be re-written in terms of degree of conversion $\alpha = ([M_0]-[M])/[M_0]$. It follows:

$$\frac{d\alpha}{dt} = k_p\left(\frac{fk_d}{k_t}\right)^{1/2}\sqrt{[I]}(1-\alpha). \quad (2)$$

Due to the complex transport phenomena occurring during MMA polymerization, the kinetic parameters are variable during the reaction. For example, a lot of effort has been devoted to correlate k_p and k_t to the degree of conversion, molecular weight, free volume or chain-end mobility [8,14,27,28,40,43,64–67]. These fundamental approaches could not be applied successfully to the case of non-isothermal conditions, which are instead commonly used in the industrial practice.

Indeed, during monomer conversion the viscosity of the reaction medium markedly increases, thus the kinetic constants k_p and k_t are strongly affected not only by temperature, but also by the degree of conversion and polymerization (i.e. average length of growing macroradicals/polymer chains). Moreover, initiator efficiency drops down by several orders of magnitude as the monomer is consumed, due to the cage effect [12]. Thus, it is very important to determine the dependencies of the kinetic constants k_p and k_t and of the initiator efficiency f upon both temperature T and the degree of conversion α. Several attempts have been made in literature to find out the dependence of k_p, k_t and f on free volume, chain length, chain end mobility and, ultimately, α, but this determination is very challenging and generally less than accurate [8,27,28,40,68–71].

However, no satisfactory results in non-isothermal conditions could be obtained, or the predictions were extremely sensitive to the parameter values [24,59]. Therefore, the more successful models are still empirical or semi-empirical as reviewed by Tefera et al. [61,62]. To overcome these issues, in this work we define an overall kinetic constant depending on both T and α. In particular, it is assumed that the function of T and α is the product of two functions of one variable ($h(T)$ and $g(\alpha)$, respectively) as follows:

$$k_p\left(\frac{f}{k_t}\right)^{1/2} = h(T)g(\alpha) = K^*(T)(1-\alpha)^r\alpha^n, \quad (3)$$

where $h(T) = K^*(T)$ is a temperature-dependent rate constant, and $g(\alpha) = (1-\alpha)^r\alpha^n$ comprises the driving force of the reaction $(1-\alpha)$ and the interplay among initiation, propagation and termination constants, which are variable with solution viscosity/degree of conversion. Substituting Eq. (3) into (2), it results:

$$\frac{d\alpha}{dt} = K^*(T)\sqrt{k_d[I]}(1-\alpha)^m\alpha^n, \quad (4)$$

where $m = r+1$.

An overall kinetic constant, dependent on temperature only, can thus be introduced:

$$K(T) = K^*\sqrt{k_d}. \quad (5)$$

Thus, Eq. (4) can be re-written as:

$$\frac{d\alpha}{dt} = K(T)\sqrt{[I]}(1-\alpha)^m\alpha^n. \quad (6)$$

K, m and n are adjustable parameters; m and n are dimensionless and, as described in Section 4, are weak and linear functions of temperature, while K depends on temperature according to an Arrhenius dependence:

$$K(T) = K_0\exp\left(-\frac{E_a}{RT}\right); \quad (7)$$

K_0 is the pre-exponential factor, E_a the activation energy, R the gas constant and T the absolute temperature.

To take into account the glass and cage effects Eq. (6) can be further modified by introducing a maximum degree of conversion $\alpha_{max} < 1$. In fact, it must be considered that, when the temperature is lower than the T_g of the polymer, the monomer is not fully converted. The T_g of the reacting system increases with increasing α and, when it approaches the test temperature, the molecular mobility is strongly reduced and the system undergoes vitrification [11]. Under these conditions, the reaction rate is drastically reduced and the total monomer conversion strongly hampered. When the test temperature approaches the T_g of the fully polymerized system α_{max} approaches unity. Under these conditions, the actual driving force is $(\alpha_{max}-\alpha)$, and Eq. (6) is accordingly modified:

$$\frac{d\alpha}{dt} = K(T)\sqrt{[I]}(\alpha_{max}-\alpha)^m\alpha^n. \quad (8)$$

A linear correlation with the temperature observed has been reported [72,73]. It is:

$$\alpha_{max} = p + qT \quad \text{for } T < T_{g,max} \quad (9)$$

$$\alpha_{max} = 1 \quad \text{for } T \geq T_{g,max}$$

where $T_{g,max}$ is the glass transition temperature of the fully cured monomer.

Eq. (10) must be coupled with an expression accounting for the decomposition of each initiator, which is assumed to follow a first order kinetics [63].

$$\frac{d[I]}{dt} = -k_d[I] \quad (10)$$

Experimental observations showed that reaction takes place after an induction time t_{ind}, necessary for inhibitor depletion by reaction with the initiator [1]. Accordingly, initiator activation is modeled by a step function $u(t-t_{ind})$:

$$\frac{d[I]}{dt} = -k_d[I]u(t-t_{ind}). \quad (11)$$

Experimental evidences showed that the induction time of the reaction, which can be found experimentally, follows a pseudo-Arrhenius trend with temperature [72,73]:

$$t_{ind} = t_{ind}^0\exp\left(\frac{E_{ind}}{RT}\right). \quad (12)$$

Here t_{ind}^0 is the induction time at infinite temperature, E_{ind} the activation energy, R the gas constant and T the absolute temperature.

The decomposition constant k_d, characteristic for each initiator, showed an Arrhenius-type dependence:

$$k_d = k_d^0\exp\left(-\frac{E_d}{RT}\right); \quad (13)$$

k_d^0 and E_d/R are evaluated from half-life data (data sheet provided by the suppliers). Also $t_{1/2}$, like induction time, was found to be dependent on temperature according to a pseudo-Arrehnius law:

$$t_{1/2} = t_{1/2}^0\exp\left(\frac{E_{1/2}}{RT}\right). \quad (14)$$

Table 1
Half-life constants for Vazo® initiators.

	Vazo®52	Vazo®64	Vazo®88
$t^0_{1/2}$(s)	5.51×10^{-17}	2.65×10^{-17}	2.44×10^{-17}
$\frac{E_{1/2}}{R}$ (K)	15582	16445	17638

$t^0_{1/2}$ and $E_{1/2}/R$ for the three initiators are reported in Table 1.

Indeed, initiator concentration can be expressed as:

$$[I] = [I_0]\exp(-k_d t) \Rightarrow \frac{[I]}{[I_0]} = \exp(-k_d t); \quad (15)$$

when $t = t_{1/2}$ it is:

$$\exp(-k_d t_{1/2}) = 0.5 \Rightarrow k_d = \frac{\ln 2}{t_{1/2}}$$

Due to induction time, the concentration ratio for every initiator drops to 0.5 when $t = t_{1/2} + t_{ind}$. For this reason, the decomposition constant has to be re-written accordingly:

$$\exp[-k_d(t_{1/2} + t_{ind})] = 0.5$$

$$k_d = \frac{\ln 2}{t_{1/2} + t_{ind}}. \quad (16)$$

In summary, the kinetic model when only one initiator is used is described by Eqs. (8), (9), (11), (12), (14), (16).

The kinetic model was written also considering the presence of multiple initiators. As well known [1], the balance on the growing radicals generated by each j-th initiator (j = 52, 64, 88 for Vazo®52, Vazo®64 and Vazo®88, respectively), under the assumption of QSSA, is:

$$\frac{d[P\cdot]_j}{dt} = v_{i,j} - v_P = 2f_j k_{d,j}[I_j] - k_t[P\cdot]^2 = 0. \quad (17)$$

To take into account the presence of multiple initiators, we consider that each macroradical generated by a j-th initiator contributes to the total amount of growing chains, and the overall concentration of growing macroradicals is given by the sum of separate contributions and is set equal to zero for the QSSA:

$$\frac{d[P\cdot]}{dt} = \sum_j 2f_j k_{d,j}[I_j] - k_t[P\cdot]^2 = 0, \quad (18)$$

hence

$$[P\cdot] = \sqrt{\frac{\sum_j f_j k_{d,j}[I]_j}{k_t}}. \quad (19)$$

Substituting Eq. (19) in (1):

$$R_p = k_p[M][P\cdot] = k_p\sqrt{\frac{\sum_j f_j k_{d,j}[I]_j}{k_t}}[M] = -\frac{d[M]}{dt}. \quad (20)$$

Being

$$R_p = -[M]_0\frac{d\alpha}{dt}, \quad (21)$$

considering that

$$\alpha = \frac{[M]_0 - [M]}{[M]_0},$$

and that the actual driving force of the free radical polymerization is $(\alpha_{max} - \alpha)$, rearrangements of Eq. (20) lead to:

$$\frac{d\alpha}{dt} = k_p\sqrt{\frac{\sum_j 2f_j k_{d,j}[I]_j}{k_t}}(\alpha_{max} - \alpha) \quad (22)$$

Substituting Eqs. (3) and (5) in Eq. (22), and re-arranging the expression it results:

$$\frac{d\alpha}{dt}(\alpha, T) = \sqrt{\sum_j K_j^2(T)[I_j]\alpha^{2n_j}(\alpha_{max} - \alpha)^{2(m_j-1)}}(\alpha_{max} - \alpha). \quad (23)$$

Here $K_j(T)$, m_j and n_j are the kinetic constant and the other parameters as previously defined, for each j-th initiator I_j.

It must be considered that, when mixed initiators are used, each initiator is activated in a different time point, and this is taken into account by Eq. (12), re-written for each j-th initiator:

$$t_{ind,j} = t^0_{ind,j}\exp\left(\frac{E_{ind,j}}{RT}\right) \quad (12')$$

Likewise, Eqs. (11), (14) and (16), when re-written for each initiator are modified as follows:

$$\frac{d\left[I_j\right]}{dt} = -k_{d,j}\left[I_j\right]u\left(t - t_{ind,j}\right); \quad (11')$$

$$t_{1/2,j} = t^0_{1/2,j}\exp\left(\frac{E_{1/2,j}}{RT}\right) \quad (14')$$

$$k_{d,j} = \frac{\ln 2}{t_{1/2,j} + t_{ind,j}} \quad (16')$$

Therefore, the kinetic model when more than one initiator is present is described by the set of Eqs. (9), (11′), (12′), (14′), (16′) and (23).

It is worth to underline that the degree of conversion α and the rate of polymerization $d\alpha/dt$ were derived from DSC as described in the following. Assuming that the heat evolved during polymerization is proportional to the extent of reaction, the degree of conversion is immediately calculated as follows [72,73]:

$$\alpha(t) = \frac{\Delta H(t)}{\Delta H_{tot}}, \quad (24)$$

where ΔH_{tot} is the total heat of polymerization, calculated by integrating the total area under the DSC curve in a non-isothermal experiment, and $\Delta H(t)$ is the heat developed in a DSC experiment between the starting point and time t. Therefore, degree of conversion and rate of polymerization are obtained from $\Delta H(t)$, i.e. the heat evolved at time t, and the heat flow $d(\Delta H)/dt$, as reported in Eq. (25):

$$\frac{d\alpha}{dt} = \frac{1}{\Delta H_{tot}}\frac{d(\Delta H)}{dt}. \quad (25)$$

Isothermal DSC experiments showed that the developed heat, ΔH_{is}, is lower than ΔH_{tot}, which indicates a fraction of unreacted monomer. Thus, the maximum degree of conversion, previously defined (less than 1 in isothermal tests), can be easily calculated by:

$$\alpha_{max} = \frac{\Delta H_{is}}{\Delta H_{tot}} \quad (26)$$

DSC data can also be used to determine the induction time, which coincides with the onset of heat generation as shown, for example, in Fig. 1. Thus, isothermal tests were performed to evaluate K, m and n in presence of each single initiator and at every temperature. In particular, the experimental $d\alpha/dt$ in isothermal conditions

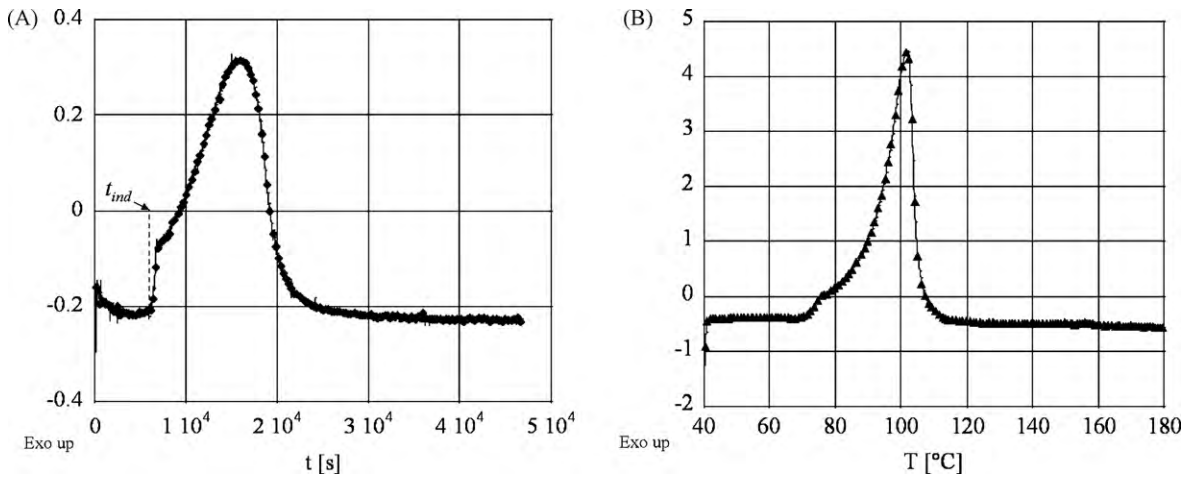

Fig. 1. Thermograms of (A) isothermal MMA polymerization, initiated with Vazo®52 at 70 °C, (B) dynamic MMA polymerization, initiated with Vazo®52. Heating rate: 0.5 °C/min.

was calculated with Eq. (25), and the corresponding experimental α obtained by integrating this equation. The results were fit by Eq. (8) using K, m and n as adjustable parameters. The trends of the adjustable parameters with temperature were determined by fitting the results at every temperature with Eqs. (7), (29) and (30) as reported in Section 4. Moreover, the experimental induction times were fit to Eq. (12). The corresponding results are reported in Table 2. Furthermore, to validate the kinetic model in non-isothermal conditions and in presence of multiple initiators, the dynamic experimental $d\alpha/dt$ and α were calculated using Eq. (25), as above described. The results were compared to the predictions of Eq. (23), without any fitting.

To estimate the importance of propagation constant and initiator efficiency compared to termination constant, the characteristic ratio fk_p^2/k_t ($1(\text{mol s})^{-1}$) can be defined, As previously published, it is [74]:

$$\frac{fk_p^2}{k_t} = \frac{R_p^2}{2k_d[I][M]^2}. \quad (27)$$

By re-arranging Eq. (27) using the kinetic model proposed in this work, the characteristic ratio can be expressed as:

$$\frac{fk_p^2}{k_t} = \frac{(d\alpha/dt)^2}{2k_d[I](1-\alpha)^2}. \quad (28)$$

4. Results and discussion

After each DSC experiment, the samples were weighed and mass loss was found to be less than 4% in each case.

To determine the kinetic parameters, isothermal tests were performed between 60 and 90 °C, every 5 °C, in presence of single initiators. For example, Fig. 1A shows the thermogram obtained when MMA was cured in presence of Vazo®52 at 70 °C. A sudden heat generation was apparent after approximately 5000 s. This indicates the induction time, which is coincident with the onset of heat generation. Induction times were determined experimentally in isothermal conditions and fit by Eq. (14). Results of the fit are listed in Table 2. The induction period of Vazo®52 was found to be rapidly decreasing with increasing temperature, which is related to the lower thermal stability of Vazo®52. Table 2 also reports $t^0_{ind,j}$ and $E_{ind,j}/R$ values, which represent the induction time at infinite temperature and the activation energy/gas constant ratio for the induction phenomenon, respectively. Fig. 1B reports the corresponding thermogram obtained during a dynamic experiment. As in isothermal experiments, an induction period can be observed. The example in Fig. 1B shows that polymerization starts at approximately 70 °C, corresponding to about 3600 s. Of course, the induction period is lower due to temperature increase during the test.

Table 2
Induction constants for Vazo® initiators.

	Vazo®52	Vazo®64	Vazo®88
t^0_{ind} (s)	8.70×10^{-17}	8.47×10^{-17}	1.58×10^{-17}
$\frac{E_{ind}}{R}$ (K)	9354	8582	8509

After each isothermal test, two dynamic scans were performed in the 40-180 °C temperature range as described in Section 2. As an example, Fig. 2 shows the thermogram obtained after the first dynamic scan following an isothermal test, by initiating MMA polymerization with Vazo®52, after isothermal test at 70 °C. A residual reactivity peak, allowing the calculation of the isothermal maximum degree of conversion, α_{max}, was detected. α_{max} is linearly dependent on temperature, as expressed in Eq. (11).

It is:

$p = 0.305$

$q = 1.88 \times 10^{-3}\ \text{K}^{-1}$

The glass transition temperatures of the partially cured polymer were obtained from the thermograms obtained by the first dynamic

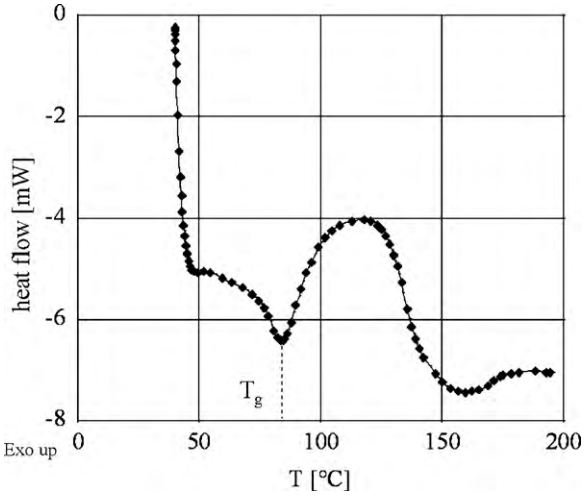

Fig. 2. DSC thermogram of the first dynamic scan after isothermal test for MMA polymerization, initiated with Vazo®52 at 70 °C.

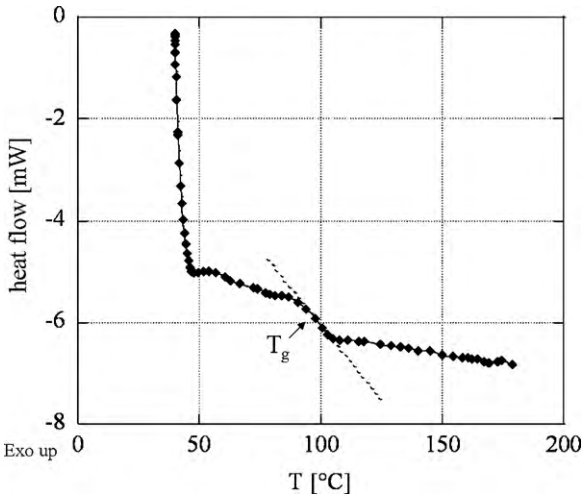

Fig. 3. DSC thermogram of the second dynamic scan after isothermal test for MMA polymerization, initiated with Vazo®52 at 70 °C.

scan. If the temperature of the isotherm is lower than 80 °C, irrespective of the initiator used, the T_g was found to exceed the isotherm temperature by 19.1 ± 3.6 °C. This difference was lower at 85 and 90 °C (13.8 ± 5.7 and 8.7 ± 2.6 °C, respectively), as the isotherm temperature approaches the maximum T_g of the fully cured polymer.

The second dynamic scan, reported in Fig. 3, shows no peak, thus indicating that the monomer is fully converted, and allowed the calculation of the T_g of the fully cured polymer from the inflection point of the DSC thermogram. T_g was found to be independent on the used initiator, and was 100.1 ± 2.6 °C.

The characteristic ratio was calculated by Eq. (28) in both isothermal and dynamic conditions, in presence of single and multiple initiators. Fig. 4 displays the plot of fk_p^2/k_t as a function of the degree of conversion α. In Fig. 4A–C are reported the results when Vazo®52, Vazo®64, Vazo®88 were used, respectively, at 60, 70, 80 and 90 °C. For α values close to 0.3 the curves are very steep, which expresses, at the very beginning of polymerization, the occurrence of gel effect, i.e. the corresponding decrease of k_t. Moreover, plots show a maximum occurring at conversions progressively increasing with increasing temperatures. At each temperature the maximum characteristic ratios were averaged on the initiators, and were found to be corresponding to degrees of conversion spanning from 0.84 ± 0.01 at 60 °C to 0.95 ± 0.02 at 90 °C. The decreasing region of the plot can be associated to the decrease of propagation constant and initiator efficiency [12,74,75].

Fig. 5 shows the characteristic ratios calculated in dynamic conditions. In Fig. 5A are reported the results in presence of single initiators for dynamic scans (40–180 °C at 0.5 °C/min, as reported in Section 2), while Fig. 5B shows the results with the contemporary presence of the three initiators. The ratios are increasing when passing from Vazo®52 to Vazo®64 to Vazo®88. This can be explained considering that Vazo®52 activates at the lowest temperature, followed by Vazo®64 and subsequently by Vazo®88. Trends with conversion are qualitatively different compared to the ones obtained with isothermal tests, because experimental temperatures reach values higher than maximum T_g of the polymer (which is around 100 °C). Therefore, polymerization occurs in a

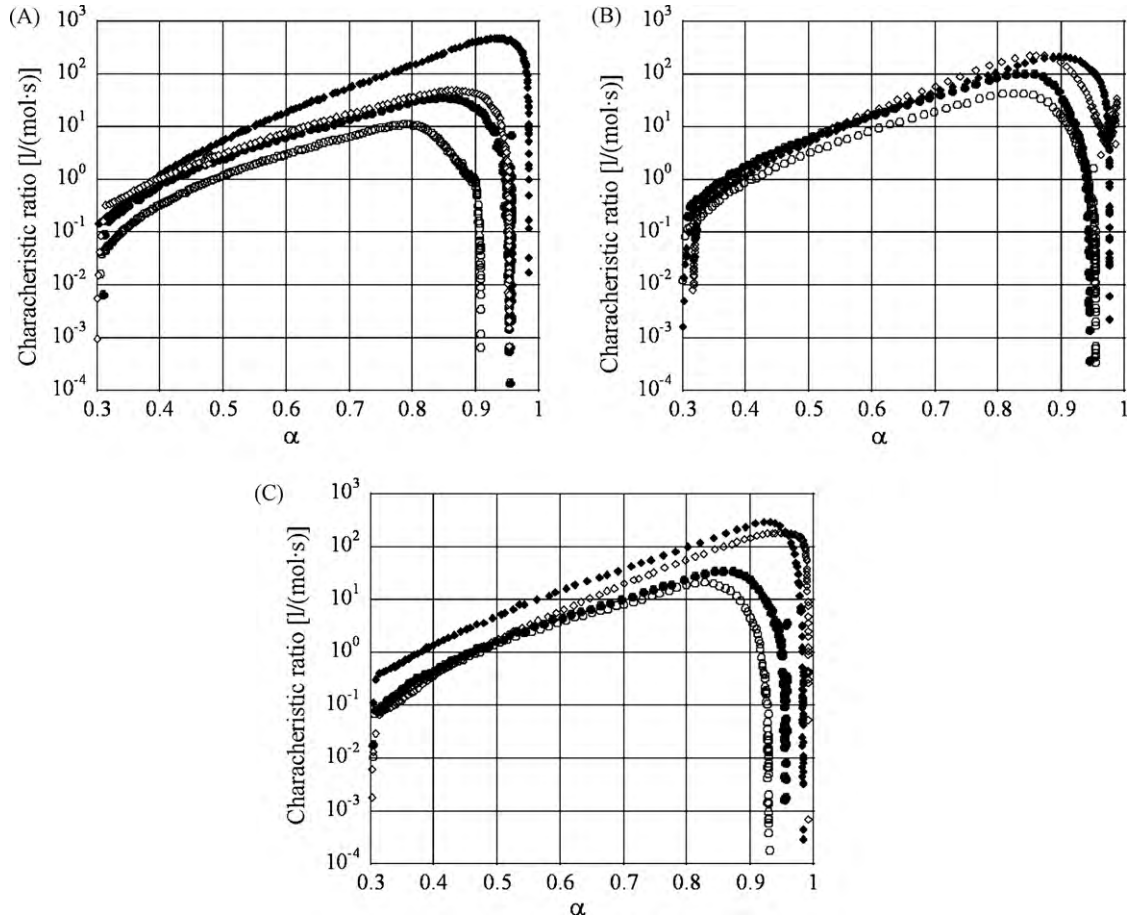

Fig. 4. Characteristic ratio fk_p^2/k_t as a function of conversion in isothermal conditions and in presence of single initiators (A) Vazo®52; (B) Vazo®64; (C) Vazo®88. Data were obtained at different temperatures: (○) 60 °C; (●) 70 °C; (◊) 80 °C; (♦) 90 °C.

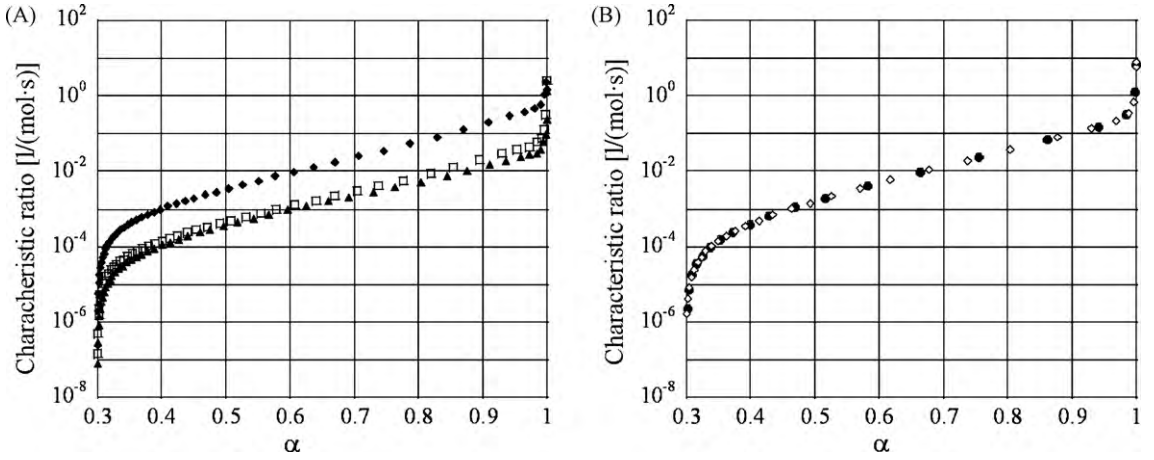

Fig. 5. Characteristic ratio fk_p^2/k_t as a function of conversion in dynamic conditions (A) in presence of single initiators; (▲): Vazo® 52; (□): Vazo® 64; (♦): Vazo® 88; (B) in presence of the three initiators (●): Vazo®52, Vazo®64 and Vazo®88; (◊)Vazo®52, Vazo®64 and Vazo®88, halved concentrations.

rubbery phase up to extreme regions of monomer conversion. In these conditions, less transport hindrances occur, and this leads to a reduced risk of uncontrolled autoacceleration. For this reason, the maximum values of the characteristic ratios are lower in dynamic conditions compared to isothermal conditions, thus confirming that diffusional effects are more important compared to thermal contributions, irrespective of the initiator. Fig. 5B shows the comparison between the characteristic ratio curves obtained when the three initiators were used, in the same concentrations of individual Vazo®s, and also halved concentrations. The plots are basically coincident, thus strongly suggesting that initiator concentration is not relevant at all in determining the importance of gel effect, though it influences the onset time of the polymerization.

DSC data were used to determine monomer conversion and rate of polymerization as a function of time in isothermal tests through Eqs. (26) and (27), respectively. Experimental results were fit by Eq. (10) with K, m and n as adjustable parameters. As an example, Figs. 6 and 7 display the experimental and fitting results for the isothermal degree of conversion and reaction rate as a function of time, when Vazo®52 is present, in the 60–90 °C range. Results obtained with the other initiators are similar. Isothermal data are fit very closely by the model (for all initiators, and at every temperature, $r^2 > 0.998$ when fitting the degree of conversion; $r^2 > 0.976$ when fitting the rate of polymerization), thus allowing accurate estimation of the adjustable parameters. It was found that K depends on temperature according to Eq. (9), while m and n are weak and linear functions of temperature, according to:

$$m = m_0 + m_1 T, \tag{29}$$

$$n = n_0 + n_1 T; \tag{30}$$

The corresponding fitting parameters K, m and n are listed in Table 3.

Dynamic experiments were carried out in the 40–180 °C range, in presence of a single initiator and co-presence of the three initiators. Fig. 8 displays the experimental dynamic degree of conversion in presence of Vazo®52, Vazo®64, Vazo®88, and in presence of the mixture of each initiator at the same concentrations used when they were individually used, while Fig. 9 displays the dynamic rate of polymerization. For all dynamic experiments, the exothermic peak was found to be sharper compared to the peak determined in isothermal conditions because increasing temperatures acceler-

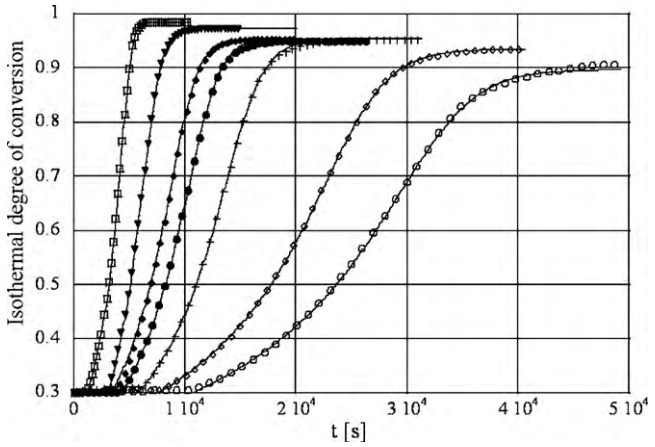

Fig. 6. Isothermal degree of conversion as a function of time in presence of Vazo®52 at different temperatures: (○) 60 °C; (◊) 65 °C; (+) 70 °C; (●) 75 °C; (♦) 80 °C; (▼) 85 °C; (□) 90 °C. Solid curves represent fitting results.

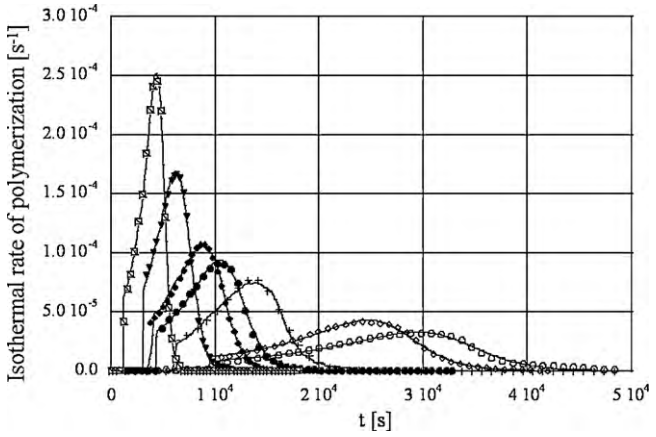

Fig. 7. Isothermal rate of polymerization as a function of time in presence of Vazo®52 at different temperatures: (○) 60 °C; (◊) 65 °C; (+) 70 °C; (●) 75 °C; (♦) 80 °C; (▼) 85 °C; (□) 90 °C. Solid curves represent fitting results.

Table 3
Polymerization constants for Vazo® initiators.

	Vazo®52	Vazo®64	Vazo®88
K_0 [$L^{1/2}/(s\,mol^{1/2})$]	1.62×10^{12}	1.43×10^{13}	1.87×10^{7}
E/R (K)	10253	10961	6612
m_0	7.00×10^{-4}	2.32×10^{-3}	4.35×10^{-3}
m_1 (K^{-1})	0.783	0.304	-0.643
n_0	0.0264	0.0323	1.25×10^{-3}
n_1 (K^{-1})	−6.06	−7.74	2.59

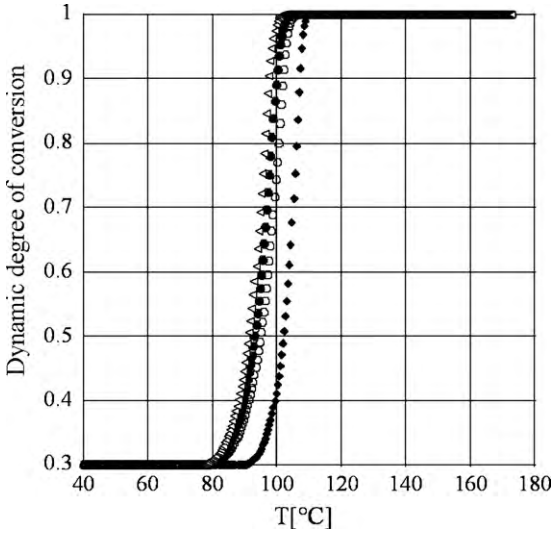

Fig. 8. Experimentally determined dynamic degree of conversion as a function of temperature with each initiator and in presence of the three initiators: (●) Vazo®52; (○) Vazo®64; (♦) Vazo®88; (▷) Vazo®52 + Vazo®64 + Vazo®88. Heating rate is 0.5 °C/min.

ate polymerization reaction. As a result, heat generation is faster, process times are shorter and the monomer is totally converted because the test is carried out up to temperatures higher than the polymer glass transition. In the case of single initiator, Vazo®52 activates at lower temperatures, followed by Vazo®64 (approximately 100 s after Vazo®52) and Vazo®88 (1400 s after Vazo®52). When Vazo®88 is used alone, the rate of polymerization curve is sharper because of the delayed activation of polymerization by Vazo®88, which shifts the whole process at higher temperatures. When the three initiators are used together, the activation temperature is very close to that for Vazo®52 (the polymerization onset in presence of the three initiators occurs 40 s before the onset with Vazo®52 used alone), which can be related to the higher overall initiator concentration. The latter leads to reduced reaction times (the polymerization is completed after 7390 s, while when Vazo®52 was used alone the time for fully converted monomer was 7830 s).

The experimental data obtained in dynamic conditions were not fit (Eq. (10)) because the model was predictive of the experimental

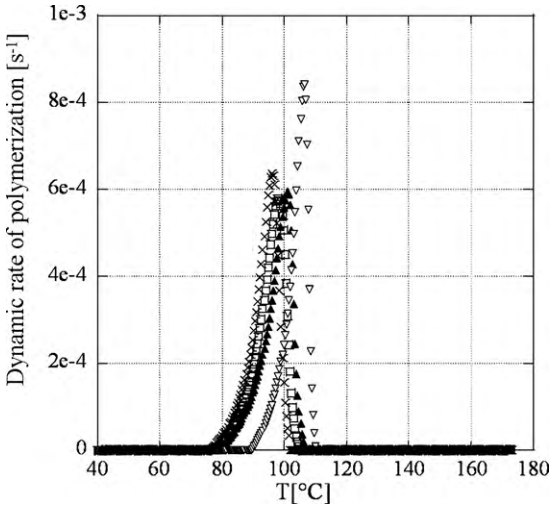

Fig. 9. Experimentally determined dynamic rate of polymerization as a function of temperature with each initiator and in presence of the three initiators: (●) Vazo®52; (○) Vazo®64; (♦) Vazo®88; (▷) Vazo®52 + Vazo®64 + Vazo®88. Heating rate is 0.5 °C/min.

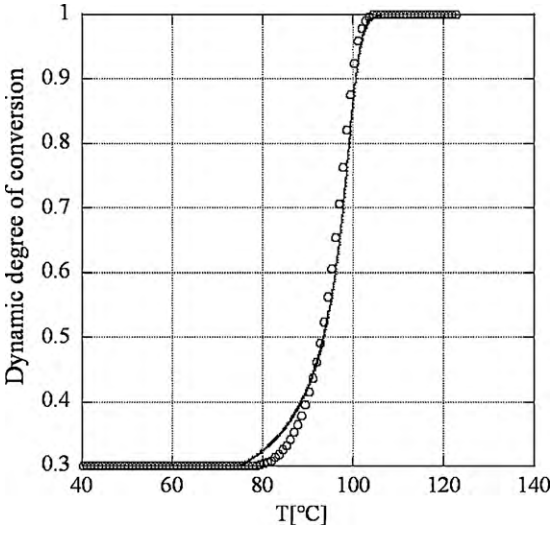

Fig. 10. Experimental data on the dynamic degree of conversion as a function of temperature in presence of Vazo®52. Solid curves represent model predictions. Heating rate is 0.5 °C/min.

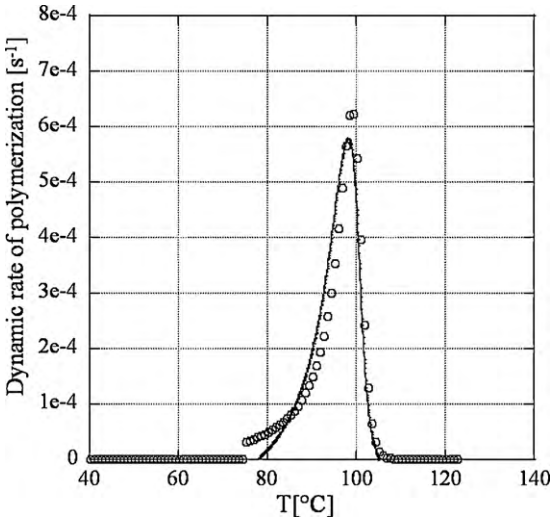

Fig. 11. Experimental data on the dynamic rate of polymerization as a function of temperature in presence of Vazo®52. Solid curves represent model predictions. Heating rate is 0.5 °C/min.

results by using the parameter values listed in Table 3 as obtained in isothermal conditions. Model predictions were compared to experimental conversion and rate of polymerization, as shown in Figs. 10 and 11 for Vazo®52, the results being similar with other single initiators. The proposed model can quantitatively predict both the degree of conversion and the rate of polymerization without any fitting. Table 4 shows the correlation factors for the comparison between the predicted and the experimentally determined

Table 4
Correlation factors between experimental results and model predictions in terms of degree of conversion and polymerization rate under dynamic conditions. Heating rate is 0.5 °C/min.

	r^2 (α)	r^2 (dα/dt)
Vazo®52	0.997	0.944
Vazo®64	0.999	0.929
Vazo®88	0.983	0.906
Vazo®52 + Vazo®64 + Vazo®88	0.992	0.842
Vazo®52 + Vazo®64 + Vazo®88, halved concentrations	0.963	0.564

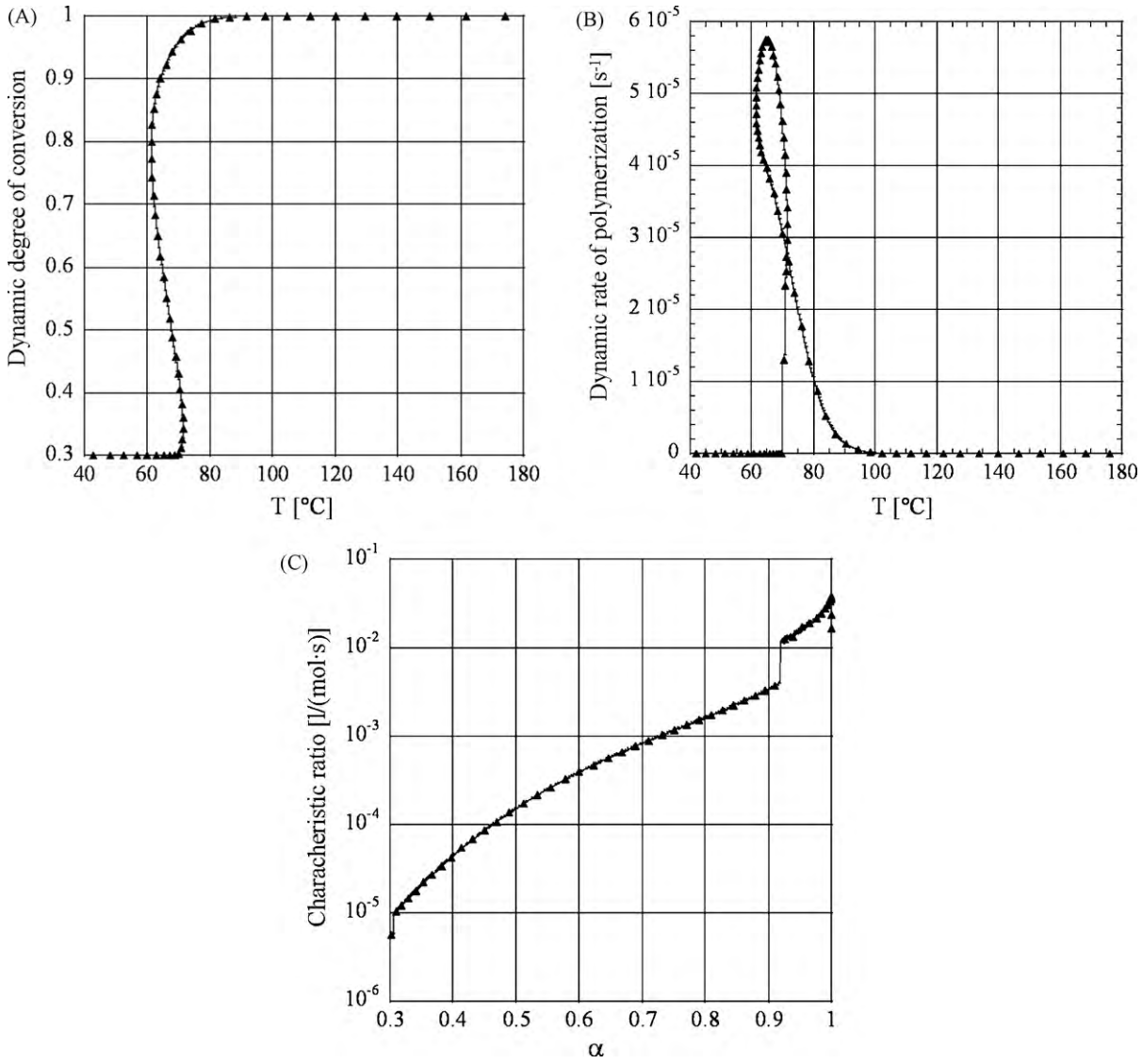

Fig. 12. Simulations obtained with a non-monotonically increasing temperature profile, as reported in Eq. (31) (A) degree of conversion; (B) rate of reaction; (C) characteristic ratio.

degree of conversion and polymerization rate. As for the conversion, model predictions are very accurate when single initiators are used, and also when the three initiators are used together. Worse results were attained for Vazo®88 and when the three initiators have been used simultaneously, but with halved concentrations. This can be ascribed to the fact that the use of Vazo®88 and of halved initiator concentrations tend to delay the onset of polymerization, i.e. to shift reaction onset at higher temperatures, when the accuracy of parameter determination is lower. In fact fitting parameters could be determined up to 90 °C, while dynamic scans get higher temperatures. Therefore, particularly in the case of Vazo®88 and mixed initiators with halved concentrations, conversion and polymerization kinetics were calculated based on extrapolated values of the parameters, thus making model predictions less reliable, in particular for extreme regions of conversions. On the other hand, the conversion history as a function of temperature is well predicted by the model, which suggests the accurate determination of the kinetic parameters associated with polymerization events.

The proposed model may be a basis to estimate the conversion and kinetic history when a random thermal history is imposed. As an example, in Fig. 12 the simulated degree of conversion/polymerization rate as a function of temperature and the characteristic ratio against conversion are plotted in the case of a non-monotonically increasing temperature. We may impose halved initiator concentrations and an arbitrary, non-monotonic temperature profile as reported in the following example:

$$T(t) = 3 \times 10^{-11} t^3 - 10^{-6} t^2 + 0.0102t + 313. \quad (31)$$

The corresponding degree of polymerization and polymerization rate are plotted in Fig. 12A and B, respectively. The characteristic ratio, as reported in Fig. 12C, reaches maximum values at least two orders of magnitude lower (0.04501 L mol^{-1} s^{-1}; Fig. 12C) compared to the values obtained when three initiators and a linear thermal history (39.8 L mol^{-1} s^{-1}; Fig. 5B) are used. This suggests that, when the polymerization is sustained by a suitable control on the temperature time trend, the importance of autoacceleration can be reduced.

5. Conclusions

In this work, a new, semi-empirical model describing the heat generation/rate of polymerization of MMA in presence of single and multiple initiators and in isothermal/dynamic conditions was developed. The model, which accounts for the presence and the

nature of different initiators, could accurately predict the experimental degree of monomer conversion and rate of polymerization in both non-isothermal conditions and in presence of multiple initiators. In particular, the importance of gel effect compared to other phenomena occurring during the conversion from monomer to polymer was evaluated under different thermal histories and initiator mixture/concentration. The results indicate that the choice of the initiator mixture and, even more importantly, of the thermal profile, may lead to an engineered kinetic guidance. The model, moreover, is simple to implement and therefore can be useful in the industrial practice as it can provide a quantitative estimate of the polymerization kinetics.

References

[1] G. Odian, Principles of Polymerization, Wiley, New York, 2004.
[2] B.M. Louie, G.M. Carratt, D.S. Soong, Modeling the free radical solution and bulk polymerization of methyl methacrylate, J. Appl. Polym. Sci. 30 (1985) 3985–4012.
[3] J.Y. Wu, G.R. Shan, Kinetic and molecular weight control for methyl methacrylate semibatch polymerization. II. Open control, J. Appl. Polym. Sci. 100 (2006) 4399–4405.
[4] V.E. Trommsdorff, H. Kohle, P. Lagally, Zur polymerisation des methacrylsauremethylesters, Makromol. Chem. 1 (1947) 169–198.
[5] R.G.W. Norrish, R.R. Smith, Catalyzed polymerization of methyl methacrylate in the liquid phase, Nature 150 (1942) 336–337.
[6] S.K. Soh, D.C. Sundberg, Diffusion-controlled vinyl polymerization. I. The gel effect, J. Polym. Sci. Polym. Chem. Ed. 20 (1982) 1299–1313.
[7] A.V. Tobolsky, C.E. Rogers, R.D. Brickman, Dead-end radical polymerization, J. Am. Chem. Soc. 82 (1960) 1277–1280.
[8] W.Y. Chiu, G.M. Carratt, D.S. Soong, A computer model for the gel effect in free-radical polymerization, Macromolecules 16 (1983) 348–357.
[9] A. Faldi, M. Tirrell, T.P. Lodge, E. von Meerwall, E. Monomer, Diffusion and the kinetics of methyl methacrylate radical polymerization at intermediate to high conversion, Macromolecules 27 (1994) 4184–4192.
[10] K. Horie, I. Mita, H. Kambe, Calorimetric investigation of polymerization reactions. I. Diffusion-controlled polymerization of methyl methacrylate and styrene, J. Polym. Sci., A-1 6 (1968) 2663–2676.
[11] I. Mita, K. Horie, Diffusion-controlled reactions in polymer systems, Rev. Macromol. Chem. Phys. 1 (1987) 91–169.
[12] G.T. Russell, D.H. Napper, R.G. Gilbert, Initiator efficiencies in high-conversion bulk polymerizations, Macromolecules 21 (1988) 2141–2148.
[13] G.D. Verros, T. Latsos, D.S. Achilias, Development of a unified framework for calculating molecular weight distribution in diffusion controlled free radical bulk homo-polymerization, Polymer 46 (2005) 539–552.
[14] G.V. Korolev, M.P. Berezin, V.P. Grachev, Free-radical vinyl polymerization in bulk: conversion dependence of initiation efficiency, Polym. Sci. Ser. A 49 (2007) 617–623.
[15] S. Terrazas-Moreno, A. Flores-Tlacuahuac, I.E. Grossmann, Simultaneous design, scheduling, and optimal control of a methyl-methacrylate continuous polymerization reactor, AIChE J. 54 (2008) 3160–3170.
[16] M Asteasuain, A. Bandoni, C. Sarmoria, A. Brandolin, Simultaneous process and control system design for grade transition in styrene polymerisation, Chem. Eng. Sci. 61 (2006) 3362–3378.
[17] A. Flores-Tlacuahuac, L.T. Biegler, Integrated control and process design during optimal polymer grade transition operations, Comput. Chem. Eng. 32 (2008) 2823–2837.
[18] A. Flores-Tlacuahuac, L.T. Biegler, Simultaneous mixed-integer dynamic optimization for integrated desgin and control, Comput. Chem. Eng. 31 (2007) 588–600.
[19] M. Rivera-Toledo, L.E. García-Crispín, A. Flores-Tlacuahuac, L. Vílchis-Ramírez, Dynamic modeling and experimental validation of the mma cell-cast process for plastic sheet production, Ind. Eng. Chem. Res. 45 (2006) 8539–8553.
[20] M. Cioffi, A.C. Hoffmann, L. Janssen, Reducing the gel effect in free radical polymerization, Chem. Eng. Sci. 56 (2001) 911–915.
[21] M. Cioffi, K.J. Ganzeveld, A.C. Hoffmann, L. Janssen, A rheokinetic study of bulk free radical polymerization performed with a helical barrel rheometer, Polym. Eng. Sci 44 (2004) 179–185.
[22] J.A. Pojman, J. Willis, D. Fortenberry, V. Ilyashenko, A.M. Khan, Factors affecting propagating fronts of addition polymerization: velocity, front curvature, temperatue profile, conversion, and molecular weight distribution, J. Polym. Sci.: Polym. Chem. 33 (1995) 643–652.
[23] W.Z Xia, W.D. Cook, Exotherm control in the thermal polymerization of nonaethylene glycol dimethacrylate (NEGDM) using a dual radical initiator system, Polymer 44 (2003) 79–88.
[24] V. Seth, S.K. Gupta, Free radical polymerizations associated with the Trommsdorff effect under semi-batch reactor conditions: an improved model, J. Polym. Eng. 15 (1995) 283–326.
[25] G.B.B. Ram, S.K. Gupta, D.N. Saraf, Free radical polymerizations associated with the Trommsdorff effect under semi-batch reactor conditions: on-line inferential state estimation, J. Appl. Polym. Sci. 64 (1997) 1861–1877.
[26] S. Garg, S.K. Gupta, D.N. Saraf, On-line optimization of free radical bulk polymerization reactors in the presence of equipment failure, J. Appl. Polym. Sci. 71 (1999) 2101–2120.
[27] D.S. Achilias, C. Kiparissides, Development of a general mathematical framework for modeling diffusion-controlled free-radical polymerization reactions, Macromolecules 25 (1992) 3739–3750.
[28] D.S. Achilias, C. Kiparissides, Modeling of diffusion-controlled free-radical polymerization reactions, J. Appl. Polym. Sci. 35 (1988) 1303–1323.
[29] G.I. Litvinenko, V.A. Kaminsky, Role of diffusion-controlled reactions in free-radical polymerization, Prog. React. Kinet. 19 (1994) 139–193.
[30] J. Gao, A. Penlidis, A Comprehensive simulator/database package for reviewing free radical homopolymerizations, J. Macromol. Sci., Rev. Macromol. Chem. Phys. 38 (1998) 651–780.
[31] C. Kiparissides, Polymerization reaction modeling: a review of recent developments and future directions, Chem. Eng. Sci. 51 (1996) 1637–1659.
[32] A. Penlidis, Polymer reaction engineering: from reaction kinetics to polymer reactor control, Can. J. Chem. Eng. 72 (1994) 385–391.
[33] D.S. Achilias, A review of modeling of diffusion controlled polymerization reactions, Macromol. Theory Simul. 16 (2007) 319–347.
[34] F.L. Marten, A.E. Hamielec, High-conversion diffusion controlled polymerizations, polymerization reactors and processes, in: J.N. Henderson, T.C. Bouton (Eds.), ACS Symposium Series, No. 104, ACS Symposium Series, Washington, DC, 1979.
[35] G. Johnston-Hall, M.J. Monteiro, Kinetic modeling of "living" and conventional free radical polymerizations of methyl methacrylate in dilute and gel regimes, Macromolecules 40 (2007) 7171–7179.
[36] K. Konstadinidis, D.S. Achilias, C. Kiparissides, Development of a unified mathematical framework for modelling molecular and structural changes in free-radical homopolymerization reactions, Polymer 33 (1992) 5019–5031.
[37] J.L. Duda, J.S. Vrentas, S.T. Ju, H.T. Liu, Prediction of diffusion coefficients for polymer-solvent systems, AIChE J. 28 (1981) 279–285.
[38] J.S. Vrentas, J.L. Duda, Molecular diffusion in polymer solutions, AIChE J. 25 (1978) 1–24.
[39] H. Fujita, A. Kishimoto, K. Matsumoto, Concentration and temperature dependence of diffusion coefficients for systems polymethyl acrylate and n-alkyl acetates, Trans. Faraday Soc. 56 (1960) 424–437.
[40] S.K. Soh, D.C. Sundberg, Diffusion-controlled vinyl polymerization. II. Limitations on the gel effect, J. Polym. Sci. Polym. Chem. Ed. 20 (1982) 1315–1329.
[41] G.A. O'Neil, M.B. Wisnudel, J.M. Torkelson, An evaluation of free volume approaches to describe the gel effect in free radical polymerization, Macromolecules 31 (1998) 4537–4545.
[42] P.G. De Gennes, Reptation of a polymer chain in the presence of fixed obstacles, J. Chem. Phys. 55 (1971) 572–579.
[43] A.W. Hui, A.E. Hamielec, Thermal polymerization of styrene at high conversions and temperatures. An experimental study, J. Appl. Polym. Sci. 16 (1972) 749–769.
[44] G.A. O'Neil, M.B. Wisnudel, J.M. Torkelson, A critical experimental examination of the gel effect in free radical polymerization: do entanglements cause autoacceleration? Macromolecules 29 (1996) 7477–7490.
[45] T. Srinivas, S. Sivakumar, K. Santosh, D.N. Gupta, Saraf, Free radical polymerizations associated with the Trommsdorff effect under semibatch reactor conditions. II: experimental responses to step changes in temperature, Polym. Eng. Sci. 36 (1996) 311–321.
[46] J.N. Cardenas, K.F. O'Driscoll, High-conversion polymerization. II. Influence of chain transfer on the gel effect, J. Polym. Sci. Polym. Chem. Ed. 15 (1977) 1883–1888.
[47] J.N. Cardenas, K.F. O'Driscoll, High-conversion polymerization. III. Kinetic behavior of ethyl methacrylate, J. Polym. Sci. Polym. Chem. Ed. 15 (1977) 2097–2108.
[48] J.T. Tulig, M. Tirrell, Molecular theory of the Trommsdorff effect, Macromolecules 14 (1981) 1501–1511.
[49] S.A. Bhat, D.N. Saraf, S. Gupta, S.K. Gupta, Use of agitator power as a soft sensor for bulk free-radical polymerization of methyl methacrylate in batch reactors, Ind. Eng. Chem. Res. 45 (2006) 4243–4255.
[50] J.S. Sangwai, S.A. Bhat, S. Gupta, D.N. Saraf, S.K. Gupta, Bulk free radical polymerizations of methyl methacrylate under non-isothermal conditions and with intermediate addition of initiator: experiments and modeling, Polymer 46 (2005) 11451–11462.
[51] J.S. Sangwai, D.N. Saraf, S.K. Gupta, Viscosity of bulk free radical polymerizing systems under near-isothermal and non-isothermal conditions, Polymer 47 (2006) 3028–3035.
[52] J.S. Sangwai, S.A. Bhat, D.N. Saraf, S.K. Gupta, An experimental study on online optimizing control of free radical bulk polymerization in a rheometer-reactor assembly under conditions of power failure, Chem. Eng. Sci. 62 (2007) 2790–2802.
[53] S. Curteanu, V. Bulacovschi, Free radical polymerization of methyl methacrylate: modeling and simulation under semibatch and nonisothermal reactor conditions, J. Appl. Polym. Sci. 74 (1999) 2561–2570.
[54] S. Curteanu, S. Ungureanu, C. Petrila, Modeling of thermal regime in free radical polymerization associated with gel and glass effects, Rev. Roum. Chim. 48 (2003) 499–509.
[55] J.Y. Wu, G.R. Shan, Kinetic and molecular weight control for methyl methacrylate semi-batch polymerization. I. Modelling, J. Appl. Polym. Sci. 100 (2006) 2838–2846.

[56] J. Ramos, A. Costoyas, J. Forcada, Kinetics of the batch cationic emulsion polymerization of styrene: a comparative study with the anionic case, J. Polym. Sci., Part A: Polym. Chem. 44 (2006) 4461–4478.
[57] Y. Wang, R.A. Hutchinson, M.F. Cunningham, A semi-batch process for nitroxide mediated radical polymerization, Macromol. Mater. Eng. 290 (2005) 230–241.
[58] V. Dua, D.N. Saraf, S. Gupta, Free-radical polymerizations associated with the Trommsdorff effect under semibatch reactor conditions. III. Experimental responses to step changes in initiator concentration, Polym. Eng. Sci. 59 (1996) 749–758.
[59] A.B. Ray, D.N. Saraf, S.K. Gupta, Free radical polymerizations associated with the Trommsdorff effect under semibatch reactor conditions I: modeling, Polym. Eng. Sci. 35 (1995) 1290–1299.
[60] F.A.N. Fernandes, Selection of a mixture of initiators for batch polymerization using neural networks, J. Appl. Polym. Sci. 98 (2005) 2088–2093.
[61] N. Tefera, G. Weickert, K.R. Westerterp, Modeling of free radical polymerization up to high conversion. I. A method for the selection of models by simultaneous parameter estimation, J. Appl. Polym. Sci. 63 (1997) 1649–1661.
[62] N. Tefera, G. Weickert, K.R. Westerterp, Modeling of free radical polymerization up to high conversion. II. Development of a mathematical model, J. Appl. Polym. Sci. 63 (1997) 1663–1680.
[63] R.E. Ibach, W.D. Ellis, Handbook of Wood Chemistry and Wood Composites, CRC Press, 2005 (Chapter 15).
[64] J. Brandrup, E.H. Immergut (Eds.), Polymer Handbook, Wiley, New York, 1963.
[65] S. Beuermann, M. Buback, T.P. Davis, R.G. Gilbert, R.A. Hutchinson, O.F. Olaj, G.T. Russell, J. Schweer, A.M. Van Herk, Critically evaluated rate coefficients for free-radical polymerization. 2. Propagation rate coefficients for methyl methacrylate, Macromol. Chem. Phys. 198 (1997) 1545–1560.
[66] S. Beuermann, M. Buback, T.P. Davis, N. García, R.G. Gilbert, R.A. Hutchinson, A. Kajiwara, M. Kamachi, I. Lacík, G.T. Russell, Critically evaluated rate coefficients for free-radical polymerization 4, Macromol. Chem. Phys. 204 (2003) 1338–1350.
[67] M. Buback, M. Egorov, A. Feldermann, Chain-length dependence of termination rate coefficients in acrylate and methacrylate homopolymerizations investigated via the SP-PLP technique, Macromolecules 37 (2004) 1768–1776.
[68] J.N. Cardenas, K.F. O'Driscoll, High-Conversion Polymerization. I. Theory and Applications to Methyl Methacrylate, J. Polym. Sci., Polym. Chem. Ed. 14 (1976) 883–897.
[69] K. Arai, S.J. Saito, Simulation model for the rate of bulk polymerization over the complete course of reaction, Chem. Eng. Jpn. 9 (1976) 302–313.
[70] J.T. Tulig, M. Tirrell, On the onset of the Trommsdorff effect, Macromolecules 15 (1982) 459–463.
[71] S.K. Soh, D.C. Sundberg, Diffusion-controlled vinyl polymerization. III. Free volume parameters and diffusion-controlled propagation, J. Polym. Sci., Polym. Chem. Ed. 20 (1982) 1331–1344.
[72] A. Borzacchiello, L. Ambrosio, L. Nicolais, E.J. Harper, K.E. Tanner, W. Bonfield, Comparison between the polymerization behavior of a new bone cement and a commercial one: modeling and in vitro analysis, J. Mater. Sci. Mater. Med. 9 (1998) 835–838.
[73] A. Borzacchiello, L. Ambrosio, L. Nicolais, E.J. Harper, K.E. Tanner, W. Bonfield, Isothermal and non-isothermal polymerization of a new bone cement, J. Mater. Sci. Mater. Med. 9 (1998) 317–324.
[74] R. Sack, G.V. Schulz, G. Meyerhoff, Free radical polymerization of methyl methacrylate up to the glassy state. Rates of propagation and termination, Macromolecules 21 (1988) 3345–3352.
[75] G.T. Russell, D.H. Napper, R.G. Gilbert, Termination in free-radical polymerizing systems at high conversion, Macromolecules 21 (1988) 2133–2140.